Industrial Health 2016, **54**, 308–314

Original Article

Failure of the human lumbar motion-segments resulting from anterior shear fatigue loading

Daniel M. SKRZYPIEC[1, 2*], Katrin NAGEL[2], Kay SELLENSCHLOH[2], Anke KLEIN[3], Klaus PÜSCHEL[3], Michael M. MORLOCK[2] and Gerd HUBER[2]

[1]Leeds Institute of Rheumatic and Musculoskeletal Medicine, University of Leeds, U.K.
[2]Institute of Biomechanics, TUHH Hamburg University of Technology, Germany
[3]Department of Legal Medicine, University Medical Center Hamburg-Eppendorf, Germany

Received September 17, 2015 and accepted January 15, 2016
Published online in J-STAGE January 30, 2016

Abstract: An in-vitro experiment was designed to investigate the mode of failure following shear fatigue loading of lumbar motion-segments. Human male lumbar motion-segments (age 32–42 years, n=6) were immersed in Ringer solution at 37°C and repeatedly loaded, using a modified materials testing machine. Fatigue loading consisted of a sinusoidal shear load from 0 N to 1,500 N (750 N±750 N) applied to the upper vertebra of the motion-segment, at a frequency of 5 Hz. During fatigue experiments, several failure events were observed in the dynamic creep curves. Post-test x-ray, CT and dissection revealed that all specimens had delamination of the intervertebral disc. Anterior shear fatigue predominantly resulted in fracture of the apophyseal processes of the upper vertebrae (n=4). Exposure to the anterior shear fatigue loading caused motion-segment instability and resulted in vertebral slip corresponding to grade I and 'mild' grade II spondylolisthesis, as observed clinically.

Key words: Spine, Lumbar, Shear fatigue, Failure mode, In-vitro, Spondylolysis, Spondylolisthesis

Introduction

Whole body vibrations (WBV) experienced at the workplace are an important consideration in the origin of back pain[1, 2]. Current models used to estimate risk factors related to spinal loading due to vibrations are estimated based on a dose of compressive load[3, 4]. This is mainly because fatigue compressive load component has been recognised as the most important loading direction in the human spine (e.g.[5–7]).

Shear load however, has been identified as a contributing factor to back pain[8]. Estimates from small-weight lifting[9, 10] and pushing or pulling activities[11] indicate that shear forces can reach up to 1,600 N (at L5–S1 level) and 1,200 N (at L2–3 and L1–2 levels) respectively, with substantial contribution of bony posterior elements to shear load bearing[12, 13]. These daily life shear forces might be unlikely to cause failure when a single shear loading event is concerned, since they only reach approximately 45% of the shear strength estimated from cadaveric specimens[12]. However, frequent repetitions, such as experienced during WBV, might result in shear failure due to fatigue.

Indeed, WBV exposure of pilots in military helicopters are believed to be the cause of the reported four-fold increase in prevalence of spondylolisthesis following spondylolysis[14], which is consistent with findings from in-vitro experiments suggesting fatigue origin of spondylolysis[15, 16].

For axial loading it is known that the exposure to compressive vibrations, even considerably below the ultimate strength, can cause vertebral body failure[6, 7]; with endplate area and bone mineral density being used for estimation

*To whom correspondence should be addressed.
E-mail: d.m.s@live.co.uk

of spinal compressive fatigue life[6, 7, 17]. However, similar knowledge of shear fatigue resistance of spinal motion-segments is still scarce.

The aim of this experimental cadaveric study was to evaluate the mechanism and mode of fatigue failure in male human lumbar motion-segments exposed to anterior shear fatigue loading.

Materials and Methods

Cadaveric material and its screening

Six motion-segments (L2–3 and L4–5) from the lumbar spines of male donors (age 36–42 years) were harvested at autopsy (Department of Legal Medicine, University Medical Center Hamburg-Eppendorf (UKE), Hamburg, Germany). They were double wrapped in saline-soaked towels and stored frozen at −20°C. To exclude pathological damage of the specimens they were scanned on a computed tomography (CT) scanner (Mx8000 IDT 16, Philips Healthcare, DA Best, NL).

This study was reviewed and approved (Number: OB-018/06) by Ethikkommission der Aerztekammer, Hamburg, Germany.

Specimen preparation

Each motion-segment consisted of two vertebral bodies, an intervertebral disc (IVD), apophyseal joints and adjoining ligaments. Specimens were embedded in resin (Ureol, Huntsman Advanced Materials, Everberg, Belgium) in neutral-posture with the mid-transverse IVD plane horizontal. Up to two-thirds of the vertebral body height was embedded. To improve fixation, wood screws were inserted into both vertebral bodies and apophyseal processes. Motion-segments were kept moist with Ringer solution sprayed throughout the preparation.

Test setup

Specimens were immersed in the bath with Ringer solution and equilibrated to 37°C for approximately 30 minutes. Motion-segments were loaded on a servo-hydraulic testing machine (MTS Bionix, Eden Prairie, MN) modified to apply compressive and shear forces (Fig. 1), with corresponding displacements measured by LVDTs[7]. Three orthogonal force components were measured by a load cell (6-DOF, SN 30 031, Huppert, Herrenberg, Germany) positioned below the basin.

Test protocol

Non-destructive compressive reference measurements and non-destructive parameter tests were performed. The compressive reference measurements each consisted of three cycles of quasi-static compressive ramp loading, from 0 N to 2,000 N and back to 0 N with a frequency of 0.005 Hz. Additional compressive reference measurements were taken at the end of the non-destructive parameter tests and just before the destructive anterior shear fatigue test. The non-destructive parameter test block is not subject to this publication. However, it served as a preconditioning of the specimens. The destructive anterior shear fatigue experiments reported in the current study consisted of sinusoidal cyclic loading with a range of 0 N to 1,500 N (offset: 750 N, amplitude: 750 N) at a frequency of 5 Hz. The peak anterior shear force was within range of shear loads experienced during daily activities, and was approximately 40% of the ultimate shear strength[12]. The fatigue loading lasted until the specimen reached 18 mm of anterior displacement (five out of six specimens, Table 1). The loading was interrupted after 1,000 and 10,000 shear cycles to repeat compressive reference measurements. The shear fatigue loading regime was designed without a compressive preload. It is believed that these fundamental experiments represent the worst case scenario since higher shear loading on the posterior elements is achieved without axial preload[18].

Pooling together the different spinal levels appears to be justified, since Cyron and Hutton[16] showed that there is

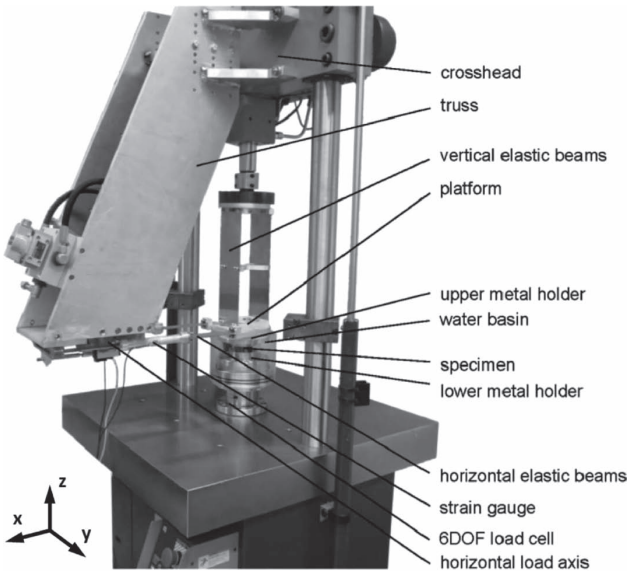

Fig. 1. Test setup and definition of coordinate system; note that additional horizontal stiffening profiles were mounted to connect truss and guiding rods to improve stiffness of the system in a horizontal direction. Anterior shear is defined as a forward displacement of upper vertebra (in positive x direction), relatively to the lower vertebra. (Figure adapted with permission from Nagel *et al.*[17])

Table 1. Overview of tested motion-segments (MS). 'Major' failure events during shear fatigue loading are underlined. #Specimen tested only up to 10 mm of anterior shear displacement. SD: standard deviation, VB: vertebral body.

Specimen description			Gross morphology			Failure						
Spinal level	Segment No	Age [yrs]	BMD (K_2HPO_4) [mg/ml]	Area (endplate) [cm^2]	IVD height [mm]	1st failure event [cycles]	2nd failure event [cycles]	3rd failure event [cycles]	4th failure event [cycles]	5th failure event [cycles]	VB slip [%]	VB slip grade [-]
L2–3	#MS-1	38	162	15.42	9.6	#3,887	-	-	-	-	n/a	-
L4–5	MS-2	39	161	14.20	9.3	30,137	35,349	38,091	-	-	28	II
L2–3	MS-3	38	110	16.90	9.8	798	1,306	1,812	-	-	12	I
L4–5	MS-4	36	189	15.65	8.5	4,725	5,261	5,736	6,566	7,139	22	I
L2–3	MS-5	42	125	16.96	9.9	20,209	24,906	27,556	-	-	13	I
L4–5	MS-6	32	179	14.77	8.6	1,863	8,818	15,347	-	-	n/a	-
Average		37	154	15.65	9.3	10,270	15,128	17,708	-	-	19	-
SD		3	31	1.11	0.6	12,045	14,428	15,117	-	-	8	-
Median		38	162	15.54	9.5	4,306	8,818	15,347	-	-	18	-

little difference in the number of fatigue cycles to failure between different lumbar vertebral levels.

Data evaluation

Based on CT scans, the trabecular bone mineral density (BMD) calibrated using a dibasic potassium phosphate phantom, was evaluated from the centre of the lower vertebral body (Avizo 5.0, VSG, Merignac, France) (Table 1). Endplate area (Area) was determined numerically (Matlab, MathWorks, Natick, MA) from the superior endplate of the lower vertebra. A detailed description of the calculation procedures is available elsewhere[7, 19]. The absolute IVD height was averaged from three measurements in the anterior, central and posterior regions of the mid-sagittal plane of the IVD (Avizo 5.0).

The last cycle from each compressive reference load-displacement data was filtered using a low pass 4th order Butterworth filter with a cut-off frequency of 0.5 Hz. From the processed compressive load-displacement data two parameters were evaluated: (1) the compressive stiffness at low compression based on the first third of data points, and (2) the compressive stiffness at high compression based on the last third of data points (Fig. 2).

Two different failure events were observed from the creep curves during shear fatigue loading: (1) increase in anterior peak displacement (one-sided discontinuity, event 2 in Fig. 3) is referred to as a 'minor' failure and (2) forward (anterior) shift of peak-to-peak displacements (two-sided discontinuity, events 1 and 3 in Fig. 3) is referred to as a 'major' failure.

Correlations between number of cycles to shear failure, BMD and Area were explored, expecting specimens with larger Area and higher BMD surviving higher number of shear cycles. A larger Area for the same loading level would result in lower stresses, and a higher BMD might indicate a stronger specimen, similarly to the results of the previous compressive fatigue experiments on the lumbar motion segments[7].

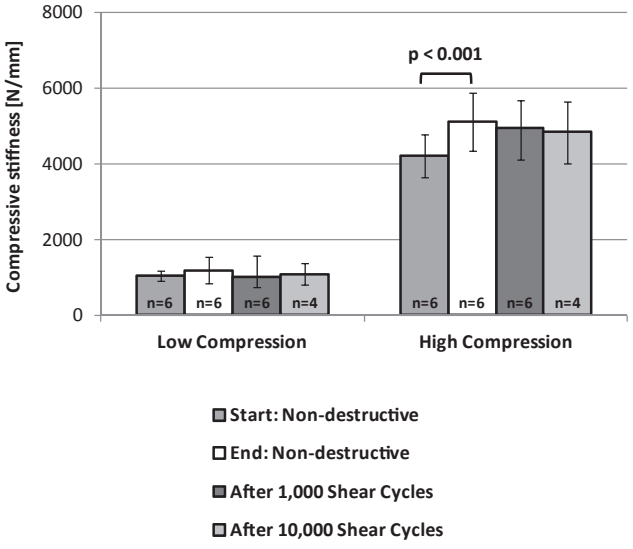

Fig. 2. Quasi-static compressive reference stiffness is lower for low compression than high compression. Generally, it remained consistent during consecutive testing within the same level of loading, apart from high compression when the compressive stiffness increased following non-destructive tests – probably due to the effect of conditioning (mean and standard deviation). Please note that for specimens MS-1 and MS-4 compressive reference measurements weren't performed after 10,000 cycles.

Post-test assessment

After mechanical testing the motion-segments were deep frozen in a geometrically fixed end-of-test position

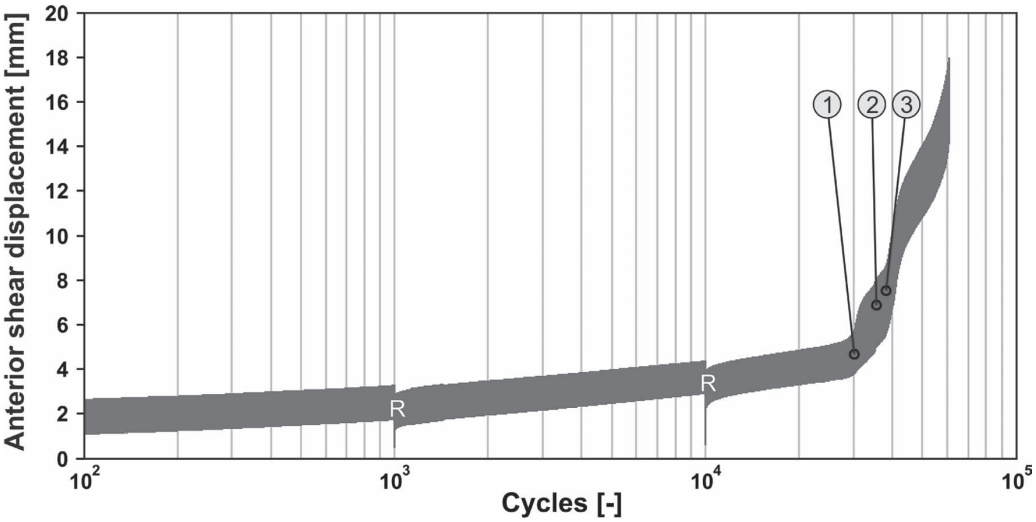

Fig. 3. Cyclic shear creep curve for the motion-segment MS-2. There are two 'major' failure events observed (1 and 3) and a 'minor' failure event (2). Note that discontinuity in the graph (R) is due to reference tests that were performed after 1,000 and 10,000 shear cycles, instead of continuous shear fatigue loading.

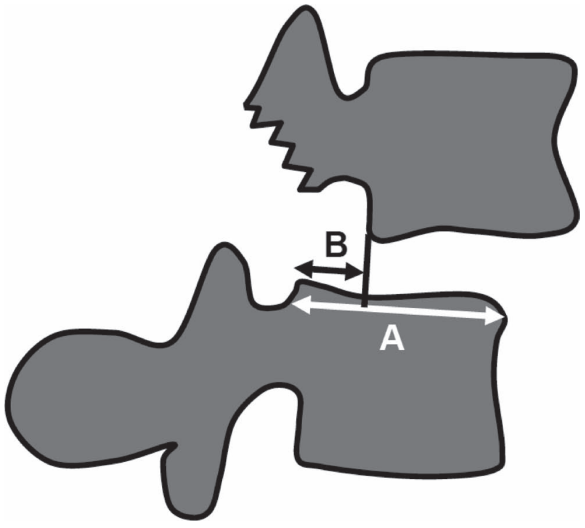

Fig. 4. Evaluation of vertebral slip as the ratio between the slip 'B' and the superior anterio-posterior length of the lower vertebral body 'A', expressed in precent[20].

(to prevent returning to neutral position after removal of shear load). This allowed visualisation of fracture of the bony elements and detachment of the IVD using x-ray images and CT scans. Vertebral slip was evaluated from X-ray images (while frozen) according to the method described by Wiltse and Winter[20] to quantify the effect of cyclic shear loading on vertebral slip progression and relate it to a clinical grade of spondylolisthesis. The severity of spondylolisthesis is graded based on the ratio of the anterior displacement of the upper vertebral body 'B' in relation to the anterio-posterior length of the lower vertebral body 'A', expressed in percent (Fig. 4): grade I up to 25%, grade II up to 50%, grade III up to 75% and grade IV up to 100%[21].

Statistical analysis

A repeated measures ANOVA was used to evaluate differences between quasi-static reference compressive stiffnesses at different stages of the experiments. Tests were performed in a statistical package (PASW 18, SPSS Inc./IBM Corporation, Armonk, NY).

Results

Compressive reference stiffness at lower compression was not significantly affected by the duration of mechanical testing ($p = 0.53$, Fig. 2). However, at high compression the compressive reference stiffness increased by 21% ($p < 0.001$, Fig. 2) following the non-destructive preconditioning and maintained small non-significant reduction during shear fatigue loading.

Over the course of the non-destructive tests, motion-segment axial height decreased by 1.51 mm on average (SD: 0.09 mm, range: 1.38 – 1.63 mm).

During the anterior shear fatigue loading, the upper vertebra crept forward due to anterior shear. Failure was accompanied by a sudden increase in anterior displacement, manifesting either as a 'minor' or a 'major' failure event (Fig. 3). The displacement diagrams of the failed specimens showed two or more changes of this kind for the five specimens tested, with up to 18 mm of anterior shear

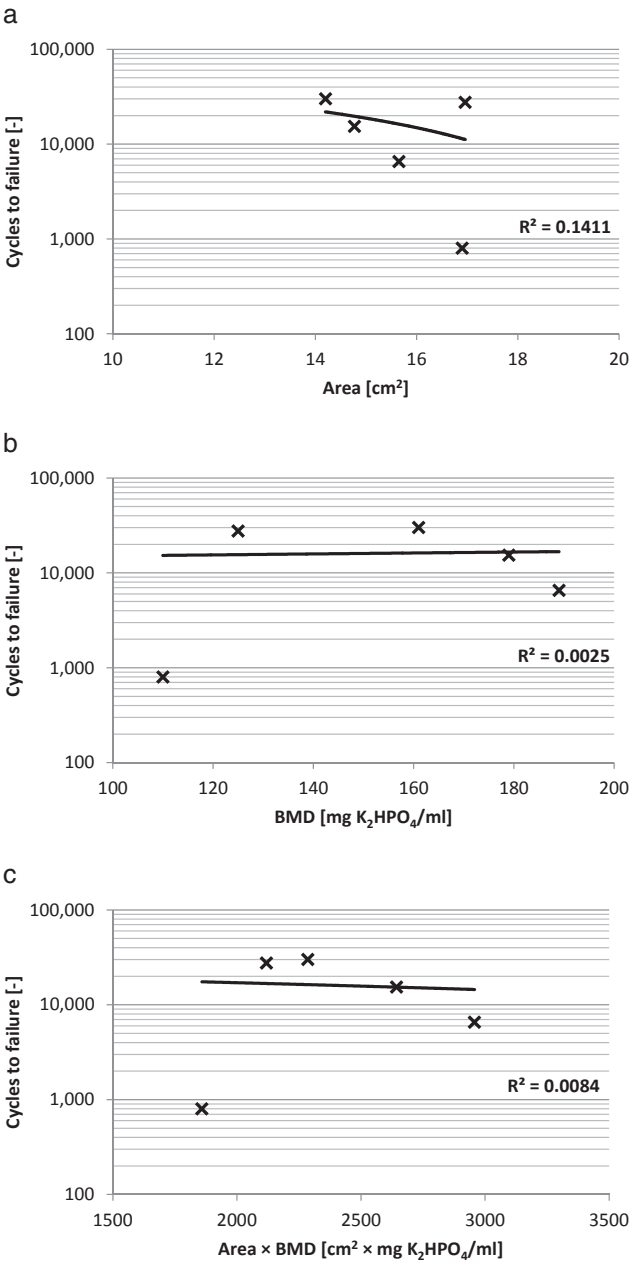

Fig. 5. Linear regression between the number of cycles to first 'major' failure and a) Area (endplate), b) BMD, c) Area × BMD cross product. Note that specimen MS-1 did not show signs of 'major' failure and was therefore not included in the analysis.

displacement (Table 1). The first segment (MS-1) was tested up to 10 mm only (Table 1), before technical modifications enabled a larger shear limit to be set. The number of cycles to the first major failure ranged between 798 cycles and 38,091 cycles (Table 1). Series of linear regressions relating number of cycles to first 'major' failure with Area ($p=0.5$, Fig. 5a), BMD ($p=0.9$, Fig. 5b) and Area × BMD product ($p=0.9$, Fig. 5c) did not show significance.

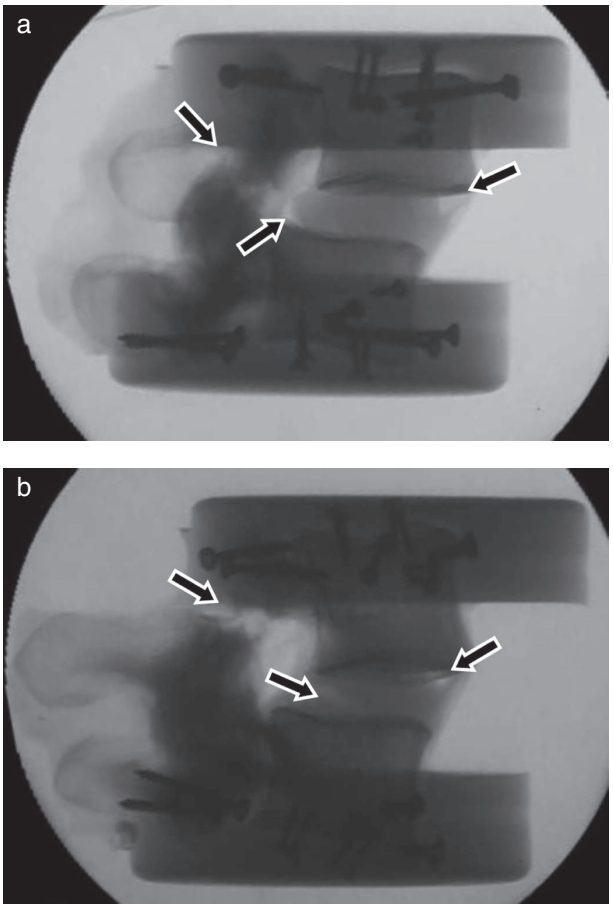

Fig. 6. X-ray images of motion-segments MS-2 (a) and MS-4 (b). Following shear fatigue tests the specimens have been frozen at the final anterior shear displacement position. Detachment of the IVD and fracture of bony posterior elements are marked with arrows. Fatigue shear tests resulted in grade II spondylolisthesis for MS-2 and grade I spondylolisthesis for MS-1 (Table 1).

Separation of the annulus from the endplates (delamination) was observed in all specimens, using post-test x-rays, CTs and dissection (Fig. 6). The posterior ligament appeared partly detached in four cases, while the anterior longitudinal ligament remained intact in all cases. Motion-segments with a 'major' failure event detected in the creep curve, sustained failure of the posterior bony elements. Subsequent dissection exposed fractures at the apophyseal processes of the upper vertebrae in four specimens and a fracture at the pedicles of the upper vertebra in one specimen.

The vertebral slip evaluated from x-ray images was observed in all but one motion-segment (Table 1). Estimated vertebral slip for four motion-segments (MS-2 to MS-5) sustaining failure of posterior elements at the upper vertebral body was 19% on average (SD: 8%), resulting in

mainly grade I spondylolisthesis with one grade II specimen (Table 1).

All but one specimen showed partially detached fixation. Particularly in one case (MS-6, Table 1), the lower vertebral body was severely damaged at the edge of the embedding material and no vertebral slip was detected.

Discussion

This study intended to decrease a gap in knowledge with regard to the mechanism and mode of fatigue failure in male human lumbar motion-segments in working age donors, subjected to anterior shear fatigue loading.

Non-destructive tests performed prior to the shear fatigue tests served as preconditioning and caused a reduction of axial height due to creep which would result in increased shear load sharing of apophyseal joints due to increased joint overlap[12].

Quasi-static compressive reference stiffness at high compression significantly increased following preconditioning, which is consistent with specimen behaviour reported by Race *et al.*[22], indicating steady state of the IVD. In addition, compressive reference stiffness was reduced only slightly by the anterior shear fatigue experiments, probably due to only two motion-segments exhibiting a major failure event below 10,000 cycles (MS-3 and MS-4) and only one of them lasting for more than 10,000 cycles (MS-3).

The neural arch of the lower lumbar levels contributes approximately 30% more to load bearing in a single overload test, than at the upper lumbar levels[13, 23]. However, there appeared to be little difference in the number of cycles to failure of the bony posterior elements in isolated L3 and L5 vertebrae reported by Cyron and Hutton[16], suggesting that the fatigue results in this study would not be significantly affected by a combination of L2–3 and L4–5 motion-segments.

In a previous shear strength study it was found that anterior shear strength correlated positively with trabecular BMD, under single overload testing conditions[12]. One would expect specimens with higher BMD to fail after many more cycles than specimens with lower BMD, but this relationship was not found (Fig. 5 b), perhaps due to the limited number of motion-segments from a relatively young and narrow age group (Table 1). In a previous compressive fatigue paper there was found a relationship between number of cycles to failure and Area × BMD product, but only for aged lumbar motion-segments with lower BMD[7]. This suggests that it might be necessary to perform the anterior shear fatigue experiments with more lumbar motion-segments from a wider age group and within wider BMD range. However, it might appear that there are different parameters required for correlation since the failing structures and the failure mechanism following shear fatigue loading might differ significantly.

The ‘major’ and ‘minor’ failure events that occurred during the shear fatigue loading were evaluated from the cyclic shear creep curves (e.g. Fig. 3). The motion-segments exhibiting ‘major’ failure events coincidentally showed damage to bony posterior elements. This can suggest that the ‘major’ failure events were signs of hard tissue failure and ‘minor’ events were related to soft tissue failure. However, it is not certain which failure event was attributable to which particular part of the motion-segment since the experiments were designed to continue until the maximum displacement was achieved and were not terminated just after a particular failure event had happened.

Spondylolytic fractures were accompanied by detached fixation of the specimens. This probably did not have an important influence on the determined failure mode, since the force control remained stable resulting in minimally altered cyclic profile to which the specimens were exposed to.

Experimental spondylolytic failure due to anterior shear fatigue loading occurred predominantly (n = 4) at the inferior apophyseal processes of the upper vertebrae. This could be related to the fact that the lamina and spinous process of upper vertebra were partly embedded, thereby strengthening the neural arch, but being deemed necessary for motion-segment mounting. This type of fracture is rarely encountered clinically but can lead to spinal canal stenosis with a significant segmental instability[24]. Exposing more lamina of the upper vertebra would allow for initiation of pars interarticularis fracture, helping to create a more physiological mode of failure. In future studies, shear fatigue tests with smaller anterior shear loads should be applied since loads of only 40% of the shear strength were able to damage the specimens relatively quickly.

This study suggests that shear loading, within physiological range, has a major impact on fatigue life of spinal specimens. The anterior cyclic shear loading should be considered in the process of evaluation of spinal risk factor due to WBV.

Acknowledgments

This study was funded by the Federal Institute for Occupational Safety and Health (FIOSH, Berlin, Germany,

project F2059). The authors acknowledge the kind support of Birgit Wulff and Jan Kolb (both of UKE, Hamburg) in handling the specimens.

Conflict of Interest

The authors confirm that there is no conflict of interest in this manuscript.

References

1) Kumar S (2001) Theories of musculoskeletal injury causation. Ergonomics **44**, 17–47. [Medline] [CrossRef]
2) Hill TE, Desmoulin GT, Hunter CJ (2009) Is vibration truly an injurious stimulus in the human spine? J Biomech **42**, 2631–5. [Medline] [CrossRef]
3) Bovenzi M, Schust M, Menzel G, Hofmann J, Hinz B (2015) A cohort study of sciatic pain and measures of internal spinal load in professional drivers. Ergonomics **58**, 1088–102. [Medline] [CrossRef]
4) Bovenzi M, Schust M, Menzel G, Prodi A, Mauro M (2015) Relationships of low back outcomes to internal spinal load: a prospective cohort study of professional drivers. Int Arch Occup Environ Health **88**, 487–99. [Medline] [CrossRef]
5) Hansson TH, Keller TS, Spengler DM (1987) Mechanical behavior of the human lumbar spine. II. Fatigue strength during dynamic compressive loading. J Orthop Res **5**, 479–87. [Medline] [CrossRef]
6) Brinckmann P, Biggemann M, Hilweg D (1988) Fatigue fracture of human lumbar vertebrae. Clin Biomech (Bristol, Avon) **3** Suppl 1, i-S23. [Medline] [CrossRef]
7) Huber G, Skrzypiec DM, Klein A, Püschel K, Morlock MM (2010) High cycle fatigue behaviour of functional spinal units. Ind Health **48**, 550–6. [Medline] [CrossRef]
8) Norman R, Wells R, Neumann P, Frank J, Shannon H, Kerr M (1998) A comparison of peak vs cumulative physical work exposure risk factors for the reporting of low back pain in the automotive industry. Clin Biomech (Bristol, Avon) **13**, 561–73. [Medline] [CrossRef]
9) Kingma I, Bosch T, Bruins L, van Dieën JH (2004) Foot positioning instruction, initial vertical load position and lifting technique: effects on low back loading. Ergonomics **47**, 1365–85. [Medline] [CrossRef]
10) Bazrgari B, Shirazi-Adl A, Arjmand N (2007) Analysis of squat and stoop dynamic liftings: muscle forces and internal spinal loads. Eur Spine J **16**, 687–99. [Medline] [CrossRef]
11) Knapik GG, Marras WS (2009) Spine loading at different lumbar levels during pushing and pulling. Ergonomics **52**, 60–70. [Medline] [CrossRef]
12) Skrzypiec DM, Klein A, Bishop NE, Stahmer F, Püschel K, Seidel H, Morlock MM, Huber G (2012) Shear strength of the human lumbar spine. Clin Biomech (Bristol, Avon) **27**, 646–51. [Medline] [CrossRef]
13) Skrzypiec DM, Bishop NE, Klein A, Püschel K, Morlock MM, Huber G (2013) Estimation of shear load sharing in moderately degenerated human lumbar spine. J Biomech **46**, 651–7. [Medline] [CrossRef]
14) Froom P, Froom J, Van Dyk D, Caine Y, Ribak J, Margaliot S, Floman Y (1984) Lytic spondylolisthesis in helicopter pilots. Aviat Space Environ Med **55**, 556–7. [Medline]
15) Hutton WC, Stott JR, Cyron BM (1977) Is spondylolysis a fatigue fracture? Spine **2**, 202–9. [CrossRef]
16) Cyron BM, Hutton WC (1978) The fatigue strength of the lumbar neural arch in spondylolysis. J Bone Joint Surg Br **60-B**, 234–8. [Medline]
17) Nagel K, Klein A, Püschel K, Morlock MM, Huber G (2013) Dependence of spinal segment mechanics on load direction, age and gender. Bundesanstalt für Arbeitsschutz und Arbeitsmedizin, Dortmund. Forschungsprojekt F2059.
18) Gardner-Morse MG, Stokes IA (2003) Physiological axial compressive preloads increase motion segment stiffness, linearity and hysteresis in all six degrees of freedom for small displacements about the neutral posture. J Orthop Res **21**, 547–52. [Medline] [CrossRef]
19) Seidel H, Pöpplau BM, Morlock MM, Püschel K, Huber G (2008) The size of lumbar vertebral endplate areas-Prediction by anthropometric characteristics and significance for fatigue failure due to whole-body vibration. Int J Ind Ergon **38**, 844–55. [CrossRef]
20) Wiltse LL, Winter RB (1983) Terminology and measurement of spondylolisthesis. J Bone Joint Surg Am **65**, 768–72. [Medline]
21) Li Y, Hresko MT (2012) Radiographic analysis of spondylolisthesis and sagittal spinopelvic deformity. J Am Acad Orthop Surg **20**, 194–205. [Medline] [CrossRef]
22) Race A, Broom ND, Robertson P (2000) Effect of loading rate and hydration on the mechanical properties of the disc. Spine **25**, 662–9. [Medline] [CrossRef]
23) Cyron BM, Hutton WC, Troup JD (1976) Spondylolytic fractures. J Bone Joint Surg Br **58-B**, 462–6. [Medline]
24) Koakutsu T, Morozumi N, Hoshikawa T, Ogawa S, Ishii Y, Itoi E (2012) Bilateral spondylolysis of inferior articular processes of the fourth lumbar vertebra: a case report. Ups J Med Sci **117**, 72–7. [Medline] [CrossRef]